The Journal of Immunology

# Differential Activation of Dual Promoters Alters D β2 Germline Transcription during Thymocyte Development

Ruth E. McMillan and Michael L. Sikes

*J Immunol* 2008; 180:3218-3228; ;
doi: 10.4049/jimmunol.180.5.3218
http://www.jimmunol.org/content/180/5/3218





*The Journal of Immunology* is published twice each month by
The American Association of Immunologists, Inc.,
1451 Rockville Pike, Suite 650, Rockville, MD 20852

Print ISSN: 0022-1767 Online ISSN: 1550-6606.

# Differential Activation of Dual Promoters Alters Dβ2 Germline Transcription during Thymocyte Development[1]

**Ruth E. McMillan and Michael L. Sikes[2]**

**Ag receptor genes are assembled through somatic rearrangements of V, D, and J gene segments. This process is directed in part by transcriptional enhancers and promoters positioned within each gene locus. Whereas enhancers coordinate reorganization of large chromatin stretches, promoters are predicted to facilitate the accessibility of proximal downstream gene segments. In TCR β locus, rearrangement initiates at two D-J cassettes, each of which exhibits transcriptional activity coincident with DJ rearrangement in CD4/CD8 double-negative pro-T cells. Consistent with a model of promoter-facilitated recombination, assembly of the DJβ1 cassette is dependent on a Dβ1 promoter (PDβ1) positioned immediately 5′ of the D. Assembly of DJβ2 proceeds independent from that of DJβ1, albeit with less efficiency. To gain insight into the mechanisms that selectively alter D usage, we have defined transcriptional regulation at Dβ2. We find that both DJβ cassettes generate germline messages in murine CD44$^+$CD25$^-$ double-negative 1 cells. However, transcription of unrearranged DJβ2 initiates at multiple sites 400–550 bp downstream of the Dβ2. Unexpectedly, loci from which germline promoter activity has been deleted by DJ rearrangement redirect transcription to sites immediately 5′ of the new DJβ2 joint. Our analyses suggest that 3′-PDβ2 activity is largely controlled by NF-κB RelA, whereas 5′-PDβ2 activity directs germline transcription of DJβ2 joints from initiator elements 76 bp upstream of the Dβ2 5′ recombination signal sequence. The unique organization and timing of Dβ2 promoter activity are consistent with a model in which promoter placement selectively regulates the rearrangement potential of Dβ2 during TCR β locus assembly.** ***The Journal of Immunology,*** **2008, 180: 3218–3228.**

The Ig and TCR genes are assembled through a series of highly regulated somatic rearrangements in developing B and T lymphocytes, respectively. Despite cell-specific segregation of Ig and TCR rearrangements, both types of Ag receptor genes are assembled via a conserved mechanism. For each locus, the Ag recognition domain is assembled from arrays of segments termed V, D, and J, by a single enzymatic complex, which targets recombination signal sequences (RSS)[3] that flank individual V, D, and J segments. During rearrangement, select RSS are bound by the lymphocyte-specific components of recombinase, encoded by RAG-1 and RAG-2 (1, 2), which introduce dsDNA breaks precisely at the boundaries between the RSS and their coding sequences (3). Processed coding ends are then ligated by ubiquitous double-stranded break-repair machinery to form unique coding joints.

As they mature in the thymus, T lymphocytes transition through a series of developmental stages identified by differential expression of numerous cell surface proteins, including CD4, 8, 25, and 44. Rearrangement and expression of individual TCR genes serve as obligate checkpoints during this maturation process. For example, before thymocytes express the CD4 and CD8 coreceptors, so-called double-negative (DN) cells must complete the assembly of a functional TCR β locus (*Tcrb*) gene (4). Cells that survive this period of β selection (5) progress to the CD4/CD8 double-positive (DP) stage of development, in which TCR α locus (*Tcra*) genes are assembled (6). Recombination of the *Tcrb* occurs in a stepwise fashion in DN cells, involving initial D-to-J joining at each of two cassettes that contain 1 D and 6 or 7 Js, followed by assembly of 1 DJ joint with 1 of ~20 distal V elements. Recombination of the upstream Dβ1 to its associated J elements has been detected in the earliest stage of DN thymocyte maturation, termed DN1 (CD44$^+$25$^-$) (7, 8), and accumulates through DN development. In contrast, rearrangement of the second DJ cassette was not detected in granulocyte/myelocyte clones derived from the DN1 or DN2 (CD44$^+$25$^+$) cells of an IL-2Rβ transgenic mouse (7). The potentiality that Dβ2 rearrangement initiates later in thymocyte development than does Dβ1 assembly correlates with the long-standing observation that germline Dβ2 sequences persist in the endogenous loci of TCRβ transgenic mice (9) and fetal thymocytes (10–12). Whether the persistence of germline Dβ2 sequences stems from a delay in the onset of Dβ2 rearrangement or a relative inefficiency with which the DJβ2 cassette gains recombinational accessibility, its consequence is to limit the availability of DJβ2 substrates for initial V-to-DJ recombination in DN3 (CD44$^{-,low}$25$^+$) cells.

The strict developmental programming of V(D)J recombination has been proposed to reflect programmed decondensation of the chromatin surrounding individual gene segments, thereby making them more accessible to recombinase. In support of this accessibility model, recombination has long been thought to require enhancer-driven chromatin decondensation and germline transcription (13, 14). Indeed, enhancer deletion impairs rearrangement to varying degrees in each of the Ag receptor loci (14). In *Tcrb*, recombination is strictly dependent upon the lone enhancer, *Tcrb*

Department of Microbiology, North Carolina State University, Raleigh, NC 27695

Received for publication May 31, 2007. Accepted for publication December 13, 2007.

The costs of publication of this article were defrayed in part by the payment of page charges. This article must therefore be hereby marked *advertisement* in accordance with 18 U.S.C. Section 1734 solely to indicate this fact.

[1] This work was supported by grants from the Elsa U. Pardee Cancer Foundation (2005-0069) and the North Carolina Agriculture Research Service (NC06711).

[2] Address correspondence and reprint requests to Dr. Michael L. Sikes, Department of Microbiology, North Carolina State University, P.O. Box 7615, Raleigh, NC 27695. E-mail address: mlsikes@ncsu.edu

[3] Abbreviations used in this paper: RSS, recombination signal sequence; Ct, cycle threshold; DN, double negative; DP, double positive; Eβ, *Tcrb* enhancer; *inr*, transcription initiator; IP, immunoprecipitation; PDβ, Dβ promoter; SP, single positive; *Tcra*, TCR α locus; *Tcrb*, TCR β locus; USF1, upstream stimulatory factor 1.

enhancer (E$\beta$) (15, 16), which has been shown to modulate the chromatin organization of a 35-kb domain that spans both DJC cassettes (17). Recombination of the first DJ$\beta$ cassette holds an additional requirement for the activation of an associated germline promoter, D$\beta$1 promoter (PD$\beta$1) (18, 19). Similar requirements for germline promoters in the *Tcra* (20, 21) and *IgH* loci (22) have suggested a general role for promoters in regulating the accessibility of neighboring gene segments. When PD$\beta$1 was repositioned between D$\beta$1 and J$\beta$1.1, recombination of a chromatinized TCR$\beta$ minilocus was severely attenuated (23). This sensitivity of DJ$\beta$1 recombination to moving the promoter downstream of the D, together with the role of transcription from individual *Tcra* germline promoters in targeting rearrangement of downstream J$\alpha$ elements (24), implies that the placement and timing of germline promoter activity relative to individual Ag receptor gene segments may profoundly impact patterns of gene segment usage.

To better understand the role of germline promoters in coordinating the differential usage of Ag receptor gene segments, we sought to characterize the elements that regulate germline transcription within the DJC$\beta$2 cassette. In this study, we describe two regions of promoter activity flanking the D$\beta$2 gene segment. Before rearrangement, germline transcription in $CD44^+25^-$ DN1 thymocytes is initiated at a diffuse array of start sites 400–550 bp 3′ of D$\beta$2. The sites of transcription initiation overlap a poorly organized 3′ promoter driven largely by p65 RelA binding at two NF-$\kappa$B sites immediately upstream of J$\beta$2.1. The unexpected placement of PD$\beta$2 between D$\beta$2 and J$\beta$2.1 precludes transcription through the D$\beta$2 RSS, suggesting a potential model for the inefficiency of DJ$\beta$2 assembly (9–12). We identified an additional promoter element 5′ of the D$\beta$2. This 5′-PD$\beta$2 was only revealed when sequences between the two promoters were deleted, and mirrored the redirection of transcription to consensus initiator elements immediately upstream of D$\beta$2 upon assembly of a DJ$\beta$2 joint in developing thymocytes. In light of this unique functional architecture, we speculate that differential promoter usage within the DJC$\beta$2 cassette may play a key role in coordinating the scope and timing of individual *Tcrb* rearrangements.

## Materials and Methods

### *Cell sorting*

FITC-conjugated CD8a (53-6.7) and CD25 (7D4) Abs, as well as PE-conjugated CD4 (RM4-5) and CD44 (IM7) Abs were purchased from BD Pharmingen. Thymii were isolated from 5-wk-old C57BL/6 mice, and RBC were removed by hypotonic lysis. Thymocytes were subsequently mixed with Abs to CD4 and CD8, and labeled cells were removed on magnetic beads coated with sheep Ab to rat IgG (Dynal). The remaining cells were labeled with FITC-conjugated anti-CD25 and PE-conjugated anti-CD44 Abs before sorting into $CD44^-/CD25^-$, $CD44^+/CD25^-$ (DN1), $CD44^+/CD25^+$ (DN2), and $CD44^-/CD25^+$ (DN3) cell populations on a 3 laser MoFlo cell sorter (DakoCytomation). Postsort evaluation of individual populations revealed purities of ≥93% for each of three experiments. All mouse studies described in this work were reviewed and approved by the institutional animal care and use committee at North Carolina State University.

### *RT-PCR*

Total RNA was isolated using TriReagent (Sigma-Aldrich), according to the manufacturer's recommendations. RNAs (0.5 $\mu$g) were reverse transcribed using Moloney murine leukemia virus reverse transcriptase (100 U; New England Biolabs) and oligo d(T) primers. The resultant cDNAs were amplified with 1 $\mu$mol each of primer pairs for D$\beta$1 (forward, 5′-GGCT ACCTCACTTTGATG-3′;reverse,5′-CCCCAGGCCTCTGCACTGATGT TCTGTGTG-3′), D$\beta$2 (forward, 5′-CAGTTCTGGAGGTAGATGGAGA ATG-3′; reverse, 5′-CTGTGTGACAGGTTTGGGTGAGCCCTCTG-3′), and $\beta$-actin (18) in either 10 mM Tris-Cl (pH 9), 50 mM KCl, 2 mM $MgCl_2$, 200 mM dNTPs, and 1 U of *Taq*, or 1× iQ SYBR Green Supermix (Bio-Rad). For semiquantitative PCR, reaction mixtures were amplified (94°C, 1 min; 57°C, 1 min; 72°C, 1.5 min) for 27 (actin) or 30 cycles (*Tcrb*), and the products were assessed using gel electrophoresis and Southern blotting. For real-time PCR, reaction mixtures were cycled 50 times. Quantitation of D$\beta$cDNAs was achieved by comparison of sample cycle threshold (Ct) values with those of serially diluted C57BL/6 thymus cDNA. Variations in sample loading were controlled by normalizing D$\beta$ values to values obtained for $\beta$ actin.

### *Transcript analyses*

For Northern blotting, 10 $\mu$g of total RNA was electrophoresed on 1% agarose formaldehyde gels. Duplicate $\zeta$-Probe (Bio-Rad) membranes were hybridized with probes 5′ of D$\beta$2 (1-kb *Stu*I/*Alu*NI fragment) or 3′ of D$\beta$2 (650-bp *Afl*III/*Eco*NI fragment). Relative amounts of RNA in each lane were estimated by hybridization with a probe to GAPDH.

For RNase protection, ssRNA probes were generated from a plasmid harboring a 1-kb PCR fragment spanning from 96 bp 5′ of D$\beta$2 to the J$\beta$2.1 RNA splice donor site. The plasmid was linearized with *Sma*I, and radiolabeled antisense probes were generated using the T7 polymerase in the presence of [$\alpha$-$^{32}$P]CTP. Full-length probes were purified on a 5% polyacrylamide gel, and hybridized with 50 $\mu$g of total RNA using the RPA III kit (Ambion). Hybridization products were separated by electrophoresis on a 5% polyacrylamide gel, and visualized by autoradiography.

The 5′-RACE was performed using a BD Smart Race kit (BD Biosciences), according to the manufacturer's instructions. Touchdown PCR of individual cDNAs was performed, according to the manufacturer's instructions, using a J$\beta$2.1-specific 3′ primer (5′-TAGGACGGTGAGTCGT GTCCC-3′), and replacing polymerase activity with the Phusion polymerase blend (New England Biolabs). Amplification products were cloned into pBluescript (Stratagene), and individual clones were sequenced.

### *Plasmids*

To construct luciferase plasmids, individual restriction fragments were isolated from p5′D2JJ-BS, which harbors a 2.5-kb PCR fragment spanning the D$\beta$2-J$\beta$2.1-J$\beta$2.2 region of murine *Tcrb*. Fragments were purified by gel electrophoresis and Qiaquick gel extraction columns (Qiagen). Purified fragments were blunted and inserted into the *Sma*I site of the pGL3-E$\beta$ or pGL2-enhancer vectors (R. McMillan and M. Sikes, unpublished data). The pGL3-E$\beta$ vector carries a 570-bp *Stu*I/*Nco*I fragment containing the mouse *Tcrb* enhancer, E$\beta$, inserted into a *Bam*HI site downstream of the firefly luciferase gene. Site-specific mutations were introduced into individual reporter constructs using the Quickchange II site-directed mutagenesis kit (Stratagene), according to the manufacturer's recommendations. Sequences for the oligonucleotide primers used to introduce each mutation (shown in bold) are as follows: mG3-5, 5′-GGTCTTATAACATC**CGA**G CATCTT-3′; mG3-6, 5′-TTCAGCCCTT**GCG**ATGTTAA-3′; mG3-7, 5′-GAATAGATGG**GCT**TCCGTTCCC-3′; m$\kappa$B-1, 5′-AGAATGTGAG**AT G**CCCCGGGTCT-3′; m$\kappa$B-2, 5′-AGGAAG**CGC**AGGAAAGAGG-3′.

### *EMSA*

Potential transcription factor binding sites were predicted using Transcription Elements Search Software (University of Pennsylvania). Gelshift probes to each potential site were generated by annealing equimolar amounts of complementary single-stranded oligonucleotides in 10 mM Tris-Cl (pH 7.4), 1 mM EDTA, and 50 mM NaCl. Each annealed oligonucleotide (1 ng) was labeled by Klenow-mediated fill-in of 4- to 6-base 5′ overhangs using [$\alpha$-$^{32}$P]dCTP and [$\alpha$-$^{32}$P]dATP radionucleotides. Nuclear protein extracts were prepared, as previously described (25), from untreated P5424 cells, or cells treated 4 h with either PMA (20 ng/ml) and ionomycin (1 $\mu$M), or overnight with LPS (1 $\mu$g/ml). Nuclear extracts were quantitated by Bradford protein assay (Bio-Rad) and stored at −80°C.

For binding reactions, each double-stranded oligonucleotide probe (1 ng) was incubated with 20 $\mu$g of the indicated nuclear extract for 20–30 min on ice in a binding mixture (20 $\mu$l) containing double-stranded poly(dI-dC) (2 mg), and BSA (10 mg) buffered in 20 mM HEPES (pH 7.9), 5% glycerol, 1 mM EDTA, 1% Nonidet P-40, and 5 mM DTT. For cold competition or supershift, reaction mixtures were pretreated with either unlabeled double-stranded competitor (100 ng) or Ab (1 $\mu$g) for 30 min on ice before addition of the radiolabeled probe. Abs against Sp1 (sc-59), GATA-3 (sc-268), NF-$\kappa$B p65 (sc-372), and NF-$\kappa$B p50 (sc-8414) were purchased from Santa Cruz Biotechnology. Reactions were separated on 6% nondenaturing polyacrylamide gel, and visualized by autoradiography. Sense strand sequences for wild-type oligonucleotides are as follows: G3-5, 5′-GGTCTTATAACATCTATGCATC-3′; G3-6, 5′-3′; PD$\beta$1 G3 (25); $\kappa$B-1, 5′-GAGAATGTGAGTAACC-3′; $\kappa$B-2, 5′-TTGAGGAAGG TGAGGAAAGAG-3′; Sp1, 5′-AACATGTGAGGAGGAGTCTAT-3′; NF-Y, 5′-AAGAGATTAACCAATCACGTA-3′. The IL-2R$\alpha\kappa$B double-stranded oligonucleotide was purchased from Santa Cruz Biotechnology (sc-2511).

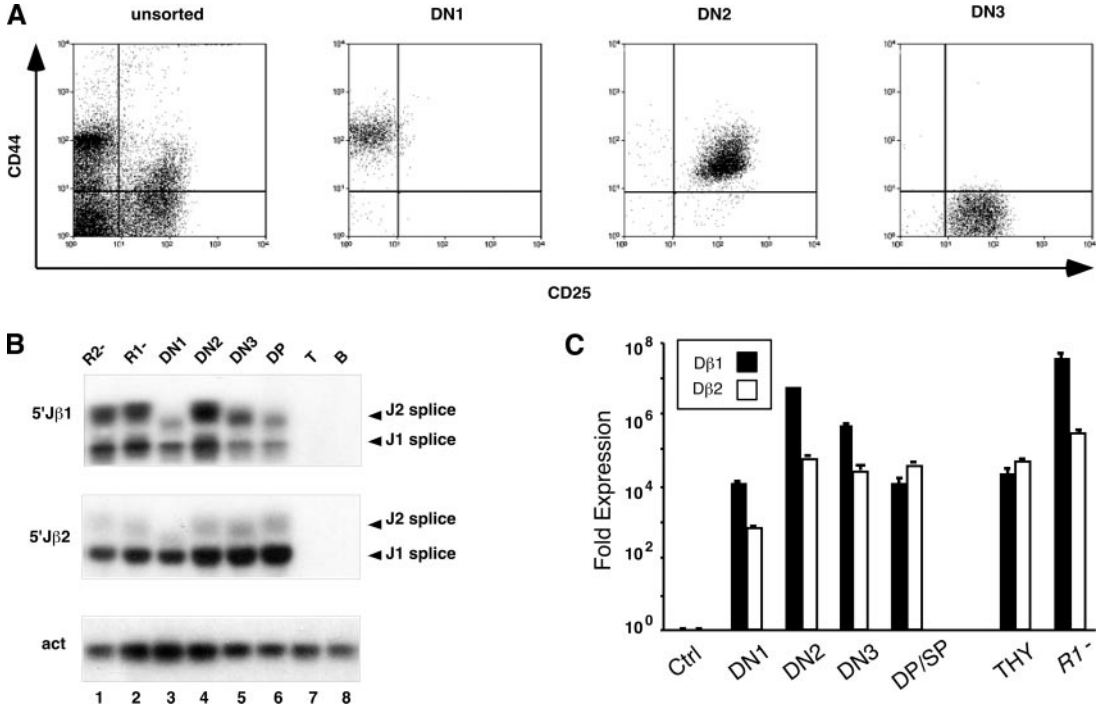


**FIGURE 1.** Developmental timing of DJβ germline transcription. *A*, Flow cytometry CD44 (*y*-axis) and CD25 (*x*-axis) expression in DN thymocytes following immunodepletion of CD4/CD8 DP and SP cells. Gates used to sort DN1 cells ($CD44^+CD25^-$), DN2 cells ($CD44^+CD25^+$), and DN3 cells ($CD44^-CD25^+$) are shown. Preparation of 30 thymii yielded $\sim 10^9$ total thymocytes, and sorted DN numbers of $0.5–2 \times 10^6$ DN1 (0.1% total), $0.3–1.1 \times 10^6$ DN2 (0.07% total), and $2–6 \times 10^6$ DN3 (0.4% total). Postsort evaluation revealed purities of 93–95% for DN2 and 96–98% for DN1 and DN3 for each of three independent sorts. *B*, RT-PCR analysis of germline transcripts that initiate 5′ of Jβ1.1 (*upper panel*) or 5′ of Jβ2.1 (*middle panel*), and splice to Cβ1 or Cβ2, respectively. $R2^-$, total RAG-$2^{-/-}$ thymocytes; $R1^-$, total RAG-$1^{-/-}$ thymocytes; T, BW5147; and B, M12 cell lines. PCR of the unrelated β-actin message (*lower panel*) served as a loading control. *C*, Quantitative real-time RT-PCR of Dβ1 (■) and Dβ2 germline transcription (□). Amplification signals were normalized for each sample ($n = 4$ replicates) to those obtained for β-actin, and expressed as fold induction above that obtained for the M12 B cell line (Ctrl). THY, unsorted C57BL/6 thymocytes.

### *Luciferase assays*

The RAG-$1^{-/-}$, $p53^{-/-}$ pro-T cell line, P5424 (26), the BW5147 mature T (27), and M12 mature B cell lines (28) have been previously described. All cell lines were cultured at 37°C/5% $CO_2$ in RPMI 1640 medium supplemented with 10% FCS, 2 mM L-glutamine, 0.01% penicillin/streptomycin, and 50 mM 2-ME. For luciferase assays, endotoxin-free (Promega PureYield) reporter plasmids were electroporated (260 V/950 μF) in P5424 cells, as described. Briefly, $10^7$ cells were washed and resuspended in 0.3 ml of serum-free RPMI 1640 along with 10 μg of individual pGL3-Eβ luciferase reporter plasmids and 0.5 μg of the control plasmid, pSV-RL (Promega). All transfections were performed three or more times with each of two independent plasmid preparations. In the absence of NF-κB induction, transfected cells were cultured for 24 h, and 50 μg of total protein from each transfectant was assayed for luciferase activity using the Dual-Luciferase Reporter system (Promega) and a Centro LB960 luminometer (Berthold Technologies). For NF-κB induction, transfected cells were cultured 40 h, divided, and cultured an additional 8 h in normal medium or medium supplemented with PMA (50 ng/ml) and ionomycin (1 μM) before harvesting.

### *Chromatin immunoprecipitation (IP) assays*

Chromatin IP reactions were performed using the ChIP-IT Express Enzyme kit (Active Motif), according to the manufacturer's instructions. Briefly, P5424 cells ($4.5 \times 10^7$) were cultured for 1 h in PMA (50 ng/ml) and ionomycin (1 μM), and transcription factor-DNA complexes were cross-linked with formldehyde and isolated chromatin was sheared by enzymatic digestion until ≥80% of DNA fragments were <500 bp in length. Protein-DNA complexes were immunoprecipitated overnight (4°C) from $10^6$ cell equivalents sheared chromatin using protein G magnetic beads and Abs (Santa Cruz Biotechnology) specific for p65 RelA (sc-109) or upstream stimulatory factor 1 (USF1) (sc-229), or with normal rabbit IgG (110-4102; Rockland Immunochemicals). Chromatin immunoprecipitates were washed, and then chromatin was eluted from the magnetic beads before cross-links were reversed and proteins were digested with proteinase K.

For real-time PCR, bound (5 μl) and input (5 μl of 1/10 dilution) samples from PMA/ionomycin-treated and untreated control cells were amplified using 1× iQ SYBR Green Supermix (Bio-Rad) and primers specific for the 5′-PDβ2 promoter (forward, 5′-CCCAAGGACATCTC CAAGCTCCTC-3′; reverse, 5′-GTTTCTTCCCCACAGGTGCCTACC-3′) or 3′-PDβ2 promoter, respectively (forward, 5′-TTACCAGTTCTGGA GGTAGATGGAG-3′; reverse, 5′-TAGGACGGTGAGTCGTGTCCC-3′). Cycling parameters for 25-μl reactions were 94°C, 30 s; 63°C, 30 s; 72°C, 30 s. Fold enrichment in the bound fractions was calculated from averages of triplicate reactions using the ΔΔCt method previously described (29), and then normalized to that obtained for the nonspecific IgG-bound fraction.

## Results

### *Developmental timing of Dβ2 recombination*

*Tcrb* recombination in developing thymocytes correlates with the appearance of sterile germline transcripts within the two DJCβ gene segment cassettes. Despite transcription within both cassettes, Dβ2-Jβ2 rearrangements have long been shown to accumulate more slowly than Dβ1-Jβ rearrangements (9–12), raising the possibility that accessibility of the Dβ2 cassette may lag behind that of the Dβ1 cassette during thymocyte development (7). To determine whether differences in DJβ recombination derive from delayed Dβ2 expression relative to Dβ1, we assessed the germline transcription status of each cassette in sorted DN subpopulations (Fig. 1). DN thymocytes account for <5% of the normal mouse thymus. After immunodepletion of DP and CD4 or eight single-positive (SP) T cells, a pool of enriched DN cells from

30 C57BL/6 thymii was sorted into $CD44^+/CD25^-$ (DN1), $CD44^+/CD25^+$ (DN2), and $CD44^-/CD25^+$ (DN3) fractions (Fig. 1*A*).

Qualitative RT-PCR readily detected germline transcription at both DJC$\beta$ cassettes in unsorted thymocytes from either RAG-$1^{-/-}$ or RAG-$2^{-/-}$ mice (Fig. 1*B*, *lanes 1* and *2*), but not in control RNA from the BW5147 T cell line (*lane 7*), in which both *Tcrb* alleles are rearranged, or in RNA from the M12 B cell line (*lane 8*). The majority of RAG-deficient thymocytes arrest as DN3 cells (30), well after the point at which D$\beta$1-J$\beta$1 recombination is first observed in wild-type DN1 cells (8). Consistent with such early D$\beta$1 recombination, we found that D$\beta$1 germline transcription was also present in wild-type DN1 cells (*upper panel*, *lane 3*), and continued throughout development (*upper panel*, *lanes 3–6*). Significantly, DN1 cells also supported transcription through the unrearranged D$\beta$2 cassette (*lower panel*, *lane 3*), suggesting that DJC$\beta$2, like DJC$\beta$1, is accessible to transcription machinery during the earliest stages of T cell development. When normalized to a B cell-negative control, real-time amplification levels for each D$\beta$ cassette (Fig. 1*C*) showed a peak in transcription through both D$\beta$ cassettes at the DN2 stage of development. Consistent with the relative inefficiency of DJ$\beta$2 recombination, germline DJ$\beta$2 transcription remained constant in later stages of development, whereas DJ$\beta$1 transcription markedly declined.

### *Initiation of D$\beta$2 germline transcription*

The D$\beta$1 promoter, PD$\beta$1, induces strong hypersensitivity to DNase I digestion (19, 31). No corresponding DNase-hypersensitive sites have been detected proximal to D$\beta$2 (32). Nonetheless, the persistence of 1.0-kb germline D$\beta$2 transcripts in mice lacking PD$\beta$1 (31) strongly suggests the presence of a D$\beta$2 promoter. We initially used Northern analyses to assess the origin of D$\beta$2 germline transcription in DN thymocytes (Fig. 2*B*). Despite abundant transcription through C$\beta$1 in both DN and DP thymocytes (R. McMillan and M. Sikes, unpublished observations), transcripts reading through sequence immediately 5′ of D$\beta$2 were only detected in DP thymocytes (*lane 2*). In contrast, a D$\beta$2 3′ probe readily detected message in RNA harvested from either RAG-$2^{-/-}$ or RAG-$2^{-/-}$PD$\beta1^{-/-}$ DN thymocytes (*lanes 3* and *4*).

Unrearranged transcripts initiating at or upstream of D$\beta$2 would yield an expected size of at least 1.6 kb. Indeed, trace amounts of 1.6-kb transcripts have previously been reported in $CD25^+/CD44^+$ thymocyte RNA (4). However, the enrichment of 1.0-kb transcripts in RAG-$2^{-/-}$ RNA (DN, Fig. 2*B*, *lane 3*) and RAG-$2^{-/-}$PD$\beta1^{-/-}$ RNA ($P1^-$, *lane 4*), together with previous studies in RAG-deficient animals (31) suggest that the bulk of D$\beta$2 germline transcripts initiates 400–600 bp 3′ of D$\beta$2. We used RNase protection (Fig. 2*C*) and 5′-RACE (Fig. 2, *D* and *E*) to separately map transcription start site within the D$\beta$2 cassette. An internally labeled 727-base antisense probe that extended from 94 bases 5′ of D$\beta$2 to the splice donor site of J$\beta$2.1 (Fig. 2*A*) protected an array of transcription start sites in separate DN RNAs (Fig. 2*C*, *lanes 3* and *4*). Sequence analysis of cloned 5′-RACE products from P5424 RNA (Fig. 2*D*, *lane 1*) corroborated this diffuse pattern of transcript initiation in DN cells. Consistent with size expectations from the Northern blots, the great preponderance of cloned start sites mapped to a 150-nt region flanking J$\beta$2.1 (Fig. 2*E*, ●). A tight cluster of start sites was mapped within the J$\beta$2.1 coding sequence. None of the cloned sites was associated with consensus TATA, transcription initiator (*inr*), or downstream promoter elements (33).

The pattern of RNase protection in DN RNA was conserved in RNA from pooled DP and SP C57BL/6 thymocytes (Fig. 2*C*, *lane 5*). Unlike transcripts observed in RAG-deficient thymocytes (Fig. 2*B*) (31), early analyses of 1.0-kb D$\beta$2 germline transcripts in wild-type mice suggested that they contained joined D$\beta$2J$\beta$2 segments (8). Our RNase protection assay revealed enrichment of multiple ~45- and ~90-base species (Fig. 2*C*, asterisks) predicted when transcripts that contain a DJ$\beta$2 joint protect the individual D$\beta$2 and J$\beta$2.1 components of our internally labeled probe. Analysis of 5′-RACE products in DP/SP RNA confirmed the presence of DJ-joined segments as well as segments harboring germline and V(D)J joints. Moreover, the bulk of start sites identified in segments carrying a D$\beta$2J$\beta$2.1 joint was positioned 100 and 104 bp 5′ of D$\beta$2 within overlapping near-consensus initiator sequences 5′-PyPyA$^{+1}$N$^{T}/_{A}$PyPy-3′ (33), whereas a single more distal start site was positioned 30 bp downstream from a perfect consensus TATA.

### *Promoter activity associated with D$\beta$2*

The differential use of start sites between germline and DJ-joined segments suggested that promoter elements might also be found both 5′ and 3′ of D$\beta$2. To identify such promoter activities, we tested the ability of fragments upstream and downstream of D$\beta$2 to direct expression of a luciferase reporter in the presence of the *Tcrb* enhancer, E$\beta$ (Fig. 3). When normalized to a promoterless control, transient transfection of a 1.65-kb *Stu*I/*Eco*RI fragment into RAG-$1^{-/-}$ P5424 DN cells yielded only 2-fold promoter activity (−1104/+563 relative to the first base of D$\beta$2), significantly less than that observed for PD$\beta$1. However, 3′ deletion of as little as 147 bp containing the majority of identified transcription start sites (−1104/+416) reduced promoter activity below that of the promoterless control. In contrast, sequential 5′ deletion of all but the 147-bp start site fragment more than doubled promoter activity (+416/+563). Similar results were obtained using the SV40 enhancer or a variety of cell lines, including the 2017 pro-T and BW5147 mature T lines (R. McMillan and M. Sikes, unpublished data).

To mimic the impact of D-to-J recombination on promoter activity, plasmids bearing further truncations to +230, +98, and −61 were assessed. In fact, a fragment entirely 5′ of D$\beta$2 (−1104/−61) exhibited promoter activity ~7.5-fold above the promoterless control. When sequence between this upstream promoter activity and the downstream 147-bp promoter was deleted or replaced with a 310-bp fragment of DNA from the bacteriophage $\phi$X174, activity from the two promoters appeared additive. From these functional assays, we conclude that D$\beta$2 is flanked by two promoter elements (5′-PD$\beta$2 and 3′-PD$\beta$2), the upstream of which may be repressed until germline sequences are deleted by D-to-J recombination.

### *NF-$\kappa$B regulates promoter activity downstream of D$\beta$2*

Potential binding sites for multiple ubiquitous and lineage-restricted transcription factors were predicted within the 1.7-kb *Stu*I/EcoR1 D$\beta$2 fragment (summarized in Fig. 4). Because germline promoter activity was restricted to sequences 3′ of D$\beta$2, we focused our initial analyses to this region that contained potential binding sites for Sp1, GATA-3, and NF-$\kappa$B. A duplex oligonucleotide probe spanning the predicted Sp1 binding site 105 bp 3′ of D$\beta$2 bound two distinct protein complexes in a P5424 nuclear protein extract (Fig. 5*A*, *lane 1*). Both complexes were specifically inhibited by competition with 100-fold excess unlabeled probe (*lane 2*), whereas mutation of the Sp1 motif severely impaired its ability to compete for protein binding (*lane 3*). The presence of Sp1 in each of the nucleoprotein complexes was confirmed by their inhibition upon addition of an Sp1-specific Ab (*lane 4*), but not upon addition of nonspecific IgG (*lane 5*). Longer exposure of the Ab reactions revealed a single Sp1-specific supershifted species (*lane 6*).

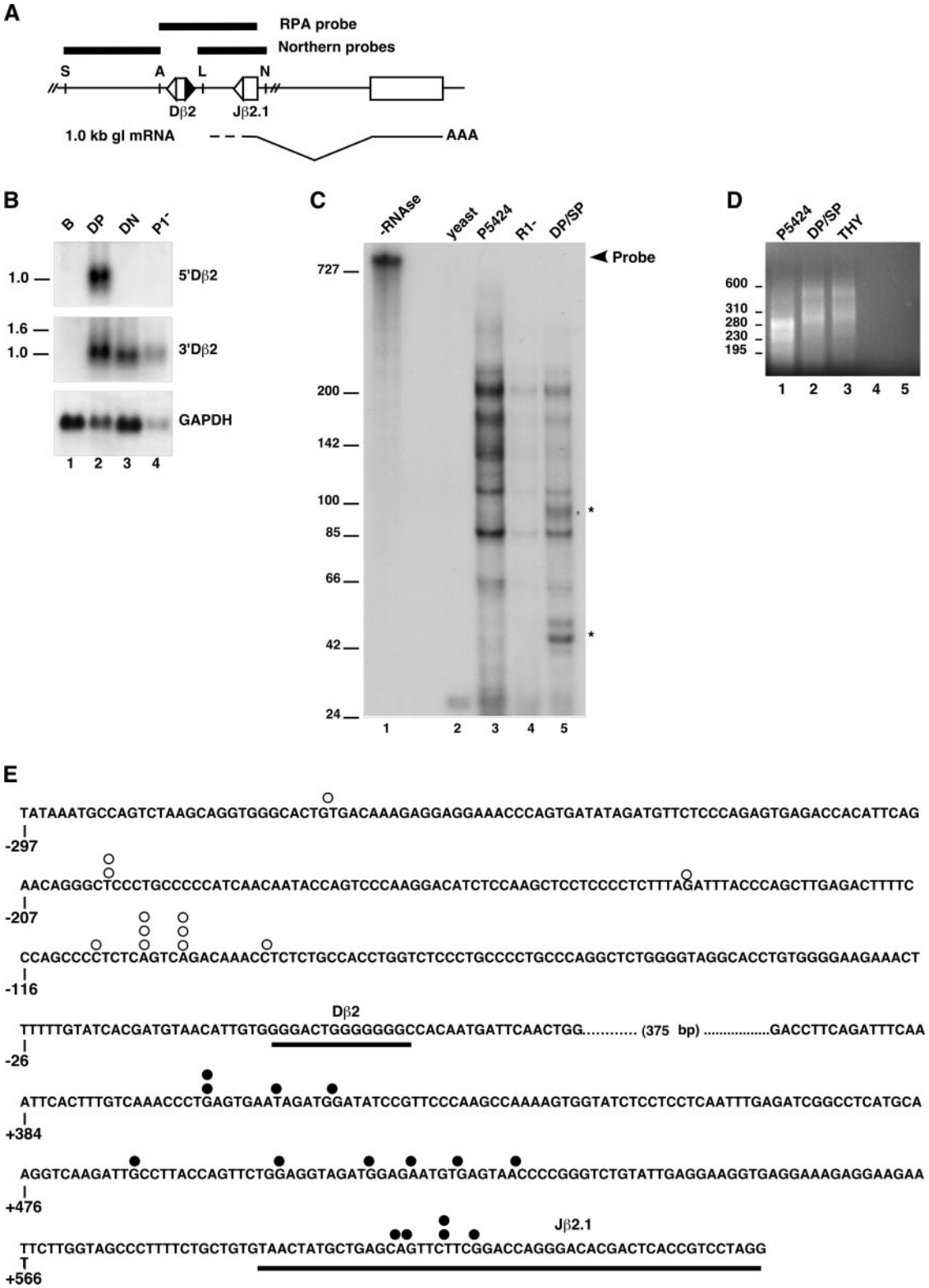


**FIGURE 2.** Initiation of Dβ2 germline transcripts. *A*, Schematic of Dβ2 region. Probes used in *B* (bars above schematic) and *C* (bar below schematic). S, *Stu*I; A, *Alu*NI; L, *Afl*III; and N, *Eco*NI. *B*, Autoradiograms of Northern hybridization with the indicated probes to RNAs from M12 (B) pooled DP and SP thymocytes (DP/SP), RAG-2$^{-/-}$ thymocytes (DN), and RAG-2$^{-/-}$PDβ1$^{-/-}$ thymocytes (P1$^{-}$). The level of GAPDH expression serves as a loading control (*lower panel*). *C*, RNase protection of a 750-base antisense probe by Dβ2 germline transcripts in RNA isolated from separate RAG-1-deficient DN sources (P5424 cells or RAG-1$^{-/-}$ thymocytes) or pooled DP/SP thymocytes. Asterisks mark protected species enriched in DP/SP RNA. *D*, Agarose gel electrophoresis of 5′-RACE products obtained from the indicated RNA sources, or from wild-type thymus in the presence of the 5′-RACE primer alone (*lane 4*) or the 3′ primer alone (*lane 5*). *E*, Map of the 5′ ends from individual RACE clones harboring germline (●) or Dβ2Jβ2.1 joined sequences (○). Dβ2 and Jβ2.1 coding sequences are underlined.

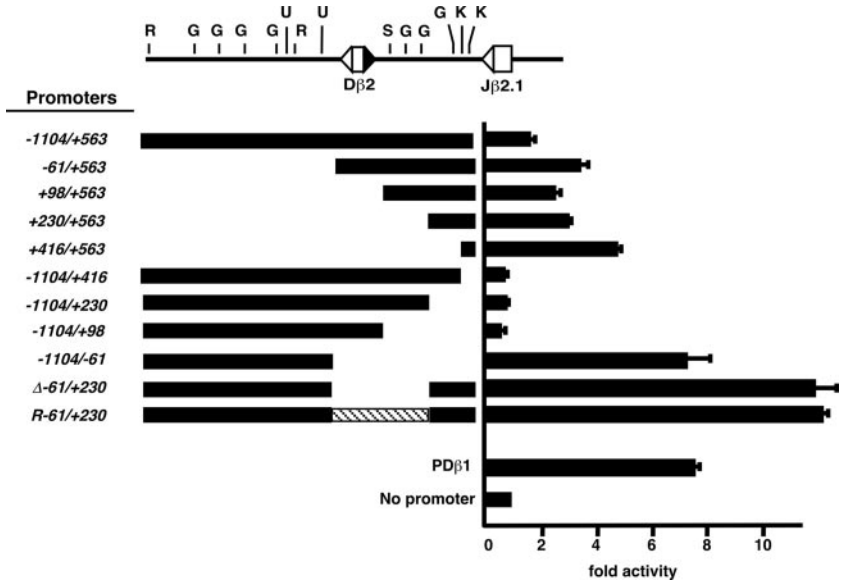


**FIGURE 3.** Promoter activities associated with D$\beta$2. The indicated DNA fragments were inserted upstream of the luciferase cassette in pGL3-E$\beta$. Fragment positioning is relative to the first base of the D$\beta$2 coding region (+1). Each plasmid was cotransfected with pSV-RL into P5424 cells, and protein extracts were assayed for luciferase activity 24 h after transfection. Values from four independent transfections were normalized to *Renilla* controls. Bars represent mean normalized luciferase activity ± SD relative to a promoterless control. Activity from the upstream PD$\beta$1 promoter is provided for comparison. Deletion or substitution of sequences between −61 and +230 in the full-length promoter fragment (−1104/+563) is respectively indicated (Δ−*61/+230*) or (*R*−*61/+230*). The positions of putative Runx (R), GATA (G), USF1 (U), Sp1 (S), and NF-κB (K) binding sites are schematized above the graph.

Binding of the T lineage-specific GATA transcription factor, GATA-3, has been demonstrated previously in both PD$\beta$1 (25, 34) and E$\beta$ (35, 36). Three separate GATA binding sites were predicted between 145 and 415 bp 3′ of D$\beta$2, although the third site contained mismatches in both bases flanking the core GATA. Separate oligonucleotide probes spanning the G3-5 and G3-6 sites formed multiple nucleoprotein complexes with P5424 protein extracts (Fig. 5*B*, *lane 1*), whereas the G3-7 site failed to demonstrate protein binding (data not shown). In each case, one major complex was fully competed and another weakly competed by an excess

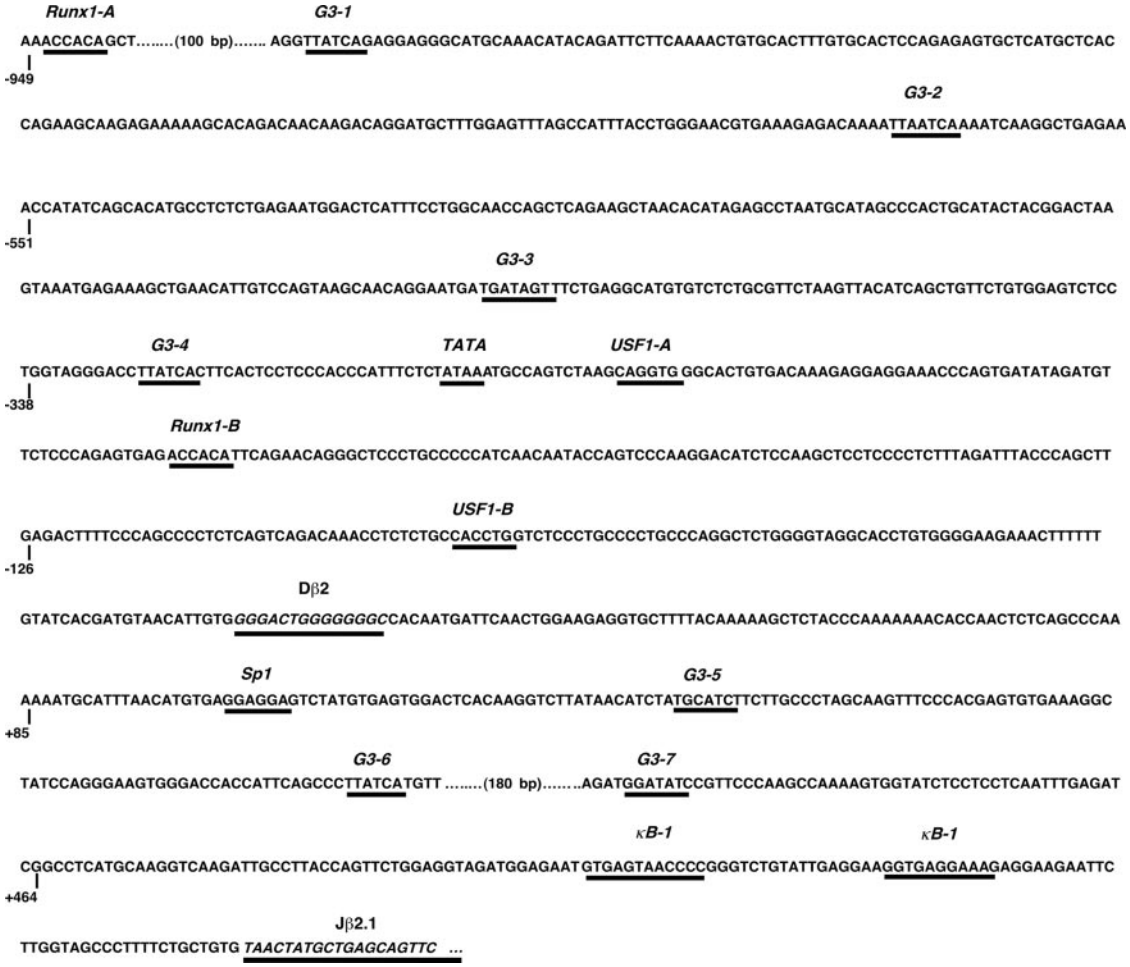


**FIGURE 4.** Organization of the D$\beta$2 regulatory region. Potential transcription factor binding sites and D$\beta$2 and J$\beta$2.1 coding sequences are shown. Numbering is relative to the first base of the D$\beta$2 coding sequence (+1). USF (USF1), G3 (GATA-3), κB (NF-κB).

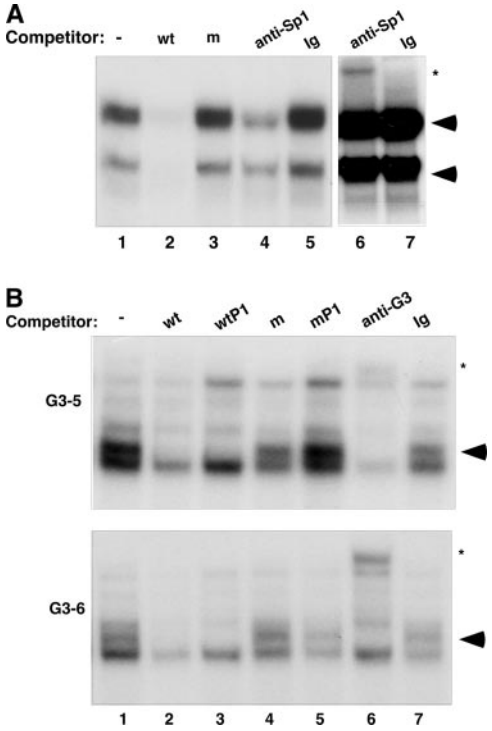


**FIGURE 5.** Sp1 and GATA-3 bind downstream of Dβ2. Nuclear extracts from the P5424 cell line were incubated with radiolabeled probes to the Sp1 (*A*) or G3-5 and G3-6 sites (*B*) alone (*lane 1*), in the presence of 100-fold molar excess of the indicated unlabeled competitors (*A*, *lanes 2* and *3*; *B*, *lanes 2–5*), or in the presence of the indicated Abs (*A*, *lanes 4–7*; *B*, *lanes 6* and *7*). Nucleoprotein complexes were resolved on a 5% acrylamide gel and visualized by autoradiography. *Lanes 6* and *7* in *A* represent longer autoradiographic exposure of *lanes 4* and *5*. Specific protein-DNA complexes (arrowheads) and Ab-supershifted complexes (asterisks) are indicated.

of unlabeled probe (*lane 2*) or a GATA-3 binding site within PDβ1 (*lane 3*). Neither oligonucleotide was effective at competing the major binding activities when its GATA core was mutated (*lanes 4* and *5*). The specificity of both primary protein complexes with G3-5 and G3-6 was confirmed by their supershift in the presence of a GATA-3 Ab, whereas other minor complexes were not specifically attenuated by the anti-GATA-3 Ab (*lane 6*).

Luciferase analyses suggested that the bulk of promoter activity 3′ of Dβ2 lies within a 147-bp span bounded by sites for the *Eco*RV and *Eco*RI restriction enzymes (Fig. 3). This fragment contains no identifiable TATA, *inr*, or downstream promoter elements. However, two potential binding sites for the NF-κB family of transcription factors are positioned proximal to the Jβ2.1 RSS (Fig. 4). Although initial gelshifts detected protein binding to probes for either of the predicted NF-κB sites using P5424 nuclear extracts (Fig. 6*A*, *lane 1*), binding was strongly induced after P5424 cells were treated for 4 h with either PMA/ionomycin (*lane 2*) or overnight with LPS (data not shown). In each case, nucleoprotein complexes were specifically inhibited by incubation with 100-fold excess unlabeled probe from either site (*lanes 3* and *6*). Binding at the downstream κB-2 probe was only weakly competed by unlabeled κB-1. Competition by either unlabeled probe was abolished upon mutation of the 3′ half-site within each putative κB motif (*lanes 4* and *5*). The specificity of each site for p65 RelA was confirmed by inhibition of each nucleoprotein complex in the presence of p65-specific Ab (*lane 8*). In contrast, nuclear protein binding to double-stranded probes containing an unrelated NF-Y binding site was unaffected by addition of anti-p65 Ab (*lower panel*, *lane 8*). Neither Abs to a second NF-κB protein, p50, nor nonspecific IgGs altered the binding pattern at either κB-1 or κB-2 (*lanes 9* and *10*).

Collectively, gelshift results indicate a complex array of transcription factor binding sites arranged between Dβ2 and Jβ2.1. In our initial reporter studies, a 320-bp region containing the Sp1, G3-5, and G3-6 binding sites was dispensable for 3′-PDβ2 promoter activity (Fig. 3). The G3-7, κB-1, and κB-2 sites are positioned within the 147-bp fragment that exhibited peak promoter activity 3′ of Dβ2. To assess the contributions of these three sites to promoter function, we selectively mutated each binding motif in the +416/+563 promoter fragment. Consistent with its failure to bind nuclear proteins in EMSA studies, mutation of the G3-7 site had no impact on promoter activity in transfected P5424 cells (Fig. 6*B*). Mutation of either NF-κB binding site, however, dramatically impaired promoter function, with luciferase activity reduced to 38 and 49% of the wild-type fragment, respectively. When both κB sites were destroyed, resultant promoter function was <20% of wild type.

Although gelshift analyses showed p65 RelA binding to the κB-1 and κB-2 sites in the nuclei of unstimulated P5424 cells (Fig. 6*A*), binding activity was markedly enhanced by PMA/ionomycin treatment. To determine whether the NF-κB-dependent activity of 3′-PDβ2 was similarly augmented, we measured the ability of transfected 3′-PDβ2 fragments to direct luciferase reporter activity in response to PMA/ionomycin. When normalized to promoter activity in untreated cells 48 h after electroporation, addition of 50 ng/ml PMA and 1 μM ionomycin during the final 8 h of culture led to a ~3-fold increase in 3′-PDβ2 activity (Fig. 6*C*). In contrast, activity of the 5′-PDβ2 promoter was not significantly affected by PMA/ionomycin treatment. Significantly, PMA/ionomycin treatment failed to rescue activity of the 3′-PDβ2 promoter when the κB-1 and κB-2 sites were destroyed. NF-κB has not, to date, been associated with activation of any of the defined *Tcr* promoters.

We next used chromatin IP to determine whether the κB-1 and κB-2 sites in 3′-PDβ2 are bound by NF-κB in vivo. P5424 cells were stimulated for 1 h with PMA/ionomycin before being treated with formaldehyde to cross-link protein-DNA complexes. Nuclear lysates were digested to enrich for mono- and dinucleosomes, and immunoprecipitated using Abs specific for RelA and USF1 and protein G magnetic beads. Purified DNA was amplified by real-time PCR using primers specific for the 3′ and 5′ Dβ2 promoters (Fig. 6*D*). The enrichment of each promoter amplicon in the bound fractions was normalized to that immunoprecipitated with total serum IgG. Although modest levels of RelA binding were detected at both the 5′ and 3′ Dβ2 promoters of untreated cells, PMA/ionomycin specifically induced a strong association of RelA with sequences that spanned the κB-1 and κB-2 sites in 3′-PDβ2. In contrast, binding of USF1 to its putative target sequences in the 5′-PDβ2 was not enhanced by PMA/ionomycin treatment. The modest increase in USF1 association with 3′-PDβ2 after PMA induction may indicate the presence of cryptic binding sites proximal to the 3′ promoter amplicon, although it most likely derives from proximity of the 5′ and 3′ promoters and the presence of larger oligonucleosome arrays in the IP reactions. Although we cannot exclude the possibility that the G3-5, G3-6, or Sp1 sites play essential roles in directing transcription through the DJβ2 cassette in developing thymocytes, our studies reveal that promoter activity in the germline sequences downstream of Dβ2 is primarily dependent on the actions of NF-κB.

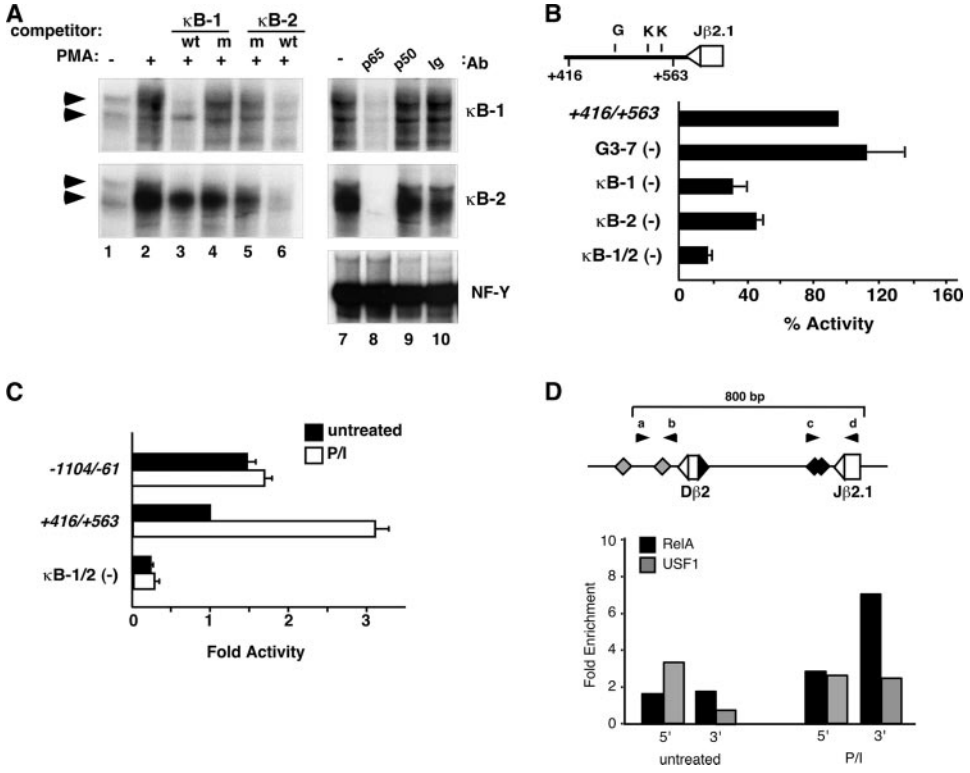


**FIGURE 6.** NF-κB contributes to promoter activity 3′ of Dβ2. *A*, Radiolabeled probes to two potential NF-κB binding sites 3′ of Dβ2 (*upper* and *middle panels*) were incubated with nuclear extracts from untreated (*lane 1*) or PMA/ionomycin-activated P5424 cells (*lanes 2–10*) alone (*lanes 2* and *7*), or in the presence of 100-fold molar excess of the indicated unlabeled competitors (*lanes 3–6*), or in the presence of the indicated Abs (*lanes 8–10*). As a control or Ab and nuclear extract quality, a radiolabeled probe to the NF-Y transcription factor was separately incubated with PMA/ionomycin-activated P5424 nuclear extract and each of the indicated Abs (*lower panel*, *lanes 7–10*). Nucleoprotein complexes were resolved on a 5% acrylamide gel and visualized by autoradiography. *B*, Individual transcription factor binding sites within the minimal downstream PDβ2 fragment (+416/+563) were selectively mutated to assess their contribution to downstream promoter activity. P5424 transfectants of the indicated mutant pGL3-Eβ (+416/+563) reporters were assessed. Results from six independent cotransfections with pSV-RL were normalized to *Renilla* levels, and expressed as percentage of that obtained for wild-type pGL3-Eβ (+416/+563). *C*, Each of the indicated luciferase reporter plasmids was transfected into P5424 cells. Transfected cells were allowed to recover for 40 h before 8-h treatment with PMA/ionomycin, and then protein extracts were assayed for luciferase activity a total of 48 h after transfection. Values from PMA/ionomycin-treated (□) and untreated controls (■) for four independent transfections were normalized to those obtained for untreated 3′-PDβ2 (+416/+563). Bars represent mean (±SEM) for *B* and *C*. *D*, Chromatin IP analyses of NF-κB RelA and USF1 association with the 5′ (*primers a* and *b*) and 3′ Dβ2 promoter sequences (*primers c* and *d*) of endogenous P5424 *Tcrb* before and after PMA/ionomycin treatment. Relative positions of the two NF-κB (◆) and predicted USF1 (gray diamonds) binding sites are indicated on the schematic diagram of the Dβ2 region. Changes in the average Ct values of triplicate amplifications for specific Ab-bound samples relative to input controls were normalized to total serum IgG and transformed to generate fold enrichment over the isotype control. The results are representative of two separate experiments.

### *Organization of promoter activity upstream of Dβ2*

Although the GATA binding sites downstream of Dβ2 appear dispensable for germline promoter activity, GATA-3 *trans* activation is essential for activation of the PDβ1 promoter (25) and Eβ (8). Motif searches of the –1104/−61 promoter fragment identified in Fig. 3 indicated a cluster of four GATA binding sites within a 415-bp stretch of sequence 5′ of Dβ2 (Fig. 4), three of which conform to the canonical GATA motif, WGATAR (37), whereas the fourth (G3-2; TGATTA) is mismatched at a single nucleotide. The promoter region upstream of Dβ2 also contains multiple potential E boxes, as well as consensus Runx binding sites at –948 and –219 (Fig. 4). The Runx family of transcription factors plays essential and diverse roles in T cell development, binding to canonical RACCRCA sites within the enhancers of all four TCR loci (38). Indeed, recent chromatin IP suggested that in addition to binding known sites in Eβ, the Runx1 protein recognizes unidentified sites flanking both Dβ1 and Dβ2 (39).

To identify the minimal 5′-PDβ2 promoter, we transfected a panel of pGL3-Eβ luciferase vectors that contained progressive deletions of the –1104/−61 promoter fragment into cultured P5424 cells. Initial 3′ deletion of 142 bp that contained the USF1-B site, both putative initiator elements, and all but one of the upstream transcription start sites identified by 5′-RACE reduced promoter activity to 37% of the –1104/−61 fragment (Fig. 7, −1104/−203). Additional 3′ deletions of 372 bp (removing all but the Runx1-A and G3-1 sites) or 520 bp (leaving only the Runx-A site) progressively attenuated promoter activity to 18 and 2% of the full-length –1104/−61 fragment, respectively. Conversely, progressive 5′ deletions had no negative effect on activity of the 5′-PDβ2 promoter. In fact, the –280/−61 fragment that lacked the Runx1-A site and all four potential GATA sites exhibited slightly higher promoter activity than the parental fragment. As such, our deletion assays suggest nominal roles for the four putative GATA elements in 5′-PDβ2 activity. Consistent with our findings, none of the putative GATA sites was detected in a search of the human Dβ2 upstream region (data not shown). Conversely, the sequence and positioning of both putative USF1 binding sites and paired initiator elements were strongly conserved. Among the two potential Runx elements, only the upstream Runx-A site was conserved between mouse and human.

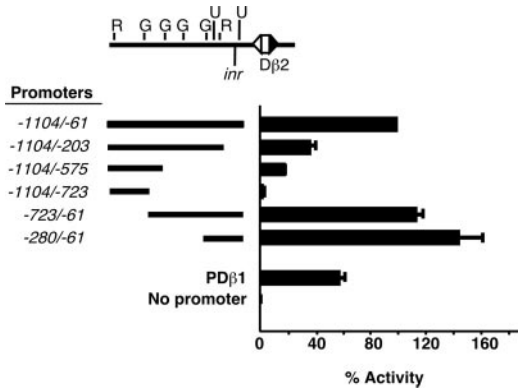


**FIGURE 7.** Promoter activity 5′ of Dβ2. The indicated DNA fragments were inserted upstream of the luciferase cassette in pGL3-Eβ. Fragment positioning is relative to the first base of the Dβ2 coding region (+1). Each plasmid was cotransfected with pSV-RL into P5424 cells, and protein extracts were assayed for luciferase activity 24 h after transfection. Results from six independent cotransfections with pSV-RL were normalized to *Renilla* levels, and expressed as percentage of that obtained for pGL3-Eβ (−1104/−61). Bars represent mean (±SEM). The positions of putative Runx (R), GATA (G), or USF1 (U) binding sites and transcription initiator (*inr*) elements are schematized above the graph.

## Discussion

A growing body of evidence has established a role for germline promoters in regulating the recombinational accessibility of discrete domains within individual Ag receptor loci. Promoters are proposed to provide a conduit through which enhancer-dependent chromatin alterations drive accessibility of promoter-proximal gene segments. Such promoter-dependent activities as recruitment of switch/sucrose nonfermentable (SWI/SNF) chromatin-remodeling complexes (40), initiation of germline transcription (24), and changes in CpG methylation (31) have all been implicated in efficient gene segment assembly. In this study, we have characterized the developmental profile of Dβ2 transcriptional activation, and have identified separate promoter activities positioned 5′ and 3′ of Dβ2. Significantly, whereas the downstream promoter appeared to direct transcription of germline Jβ2 sequences throughout DN thymocyte development, transcription from the upstream promoter was only detected in DNA harboring Dβ2Jβ2 joints. We suggest that differential activation of the two Dβ2 promoters may play a central role in coordinating the relative efficiencies with which the two DJβ cassettes are assembled.

The two Dβ2 promoters appear structurally and functionally distinct from one another. Indeed, the 3′-PDβ2 bears little homology to any of the identified TCR germline promoters, being poorly organized and with no discernable core promoter elements. The structural simplicity of 3′-PDβ2 may account for the decentralized manner of transcriptional initiation downstream of germline Dβ2. In sharp contrast, transcription directed by the 5′-PDβ2 is tightly clustered around two potential initiator elements positioned 38 bp downstream of a TTAGATT palindrome that is both a perfect match to the canonical *inr* and a single-base mismatch to the canonical TATA. Moreover, whereas activity of the upstream promoter is localized to a 340-bp sequence that contains potential binding sites for Runx1, and USF1 regulatory proteins, RelA-containing NF-κB dimers may be sufficient to drive germline transcription from the downstream promoter.

Initial analysis of promoter activity upstream of Dβ2 suggests that the four putative GATA binding sites and distal putative Runx binding site may not contribute to the activity of 5′-PDβ2 (Fig. 7). Indeed, luciferase expression in transfected cells was modestly elevated upon deletion of the Runx1-A and G3-1-to-4 sites. Recent studies by Oltz and colleagues (14) demonstrated localization of both Runx1 and GATA-3 to sequences immediately upstream of Dβ2 5′ in thymocytes of RAG-2-deficient mice, suggesting a role for Runx1 and GATA-3 in the regulation of Dβ2 usage in vivo. As such, the insensitivity of our luciferase readouts to 5′ truncations of the upstream promoter could reflect either the limitations inherent to large-scale deletion analyses and transient transfections. Alternatively, the gain in luciferase activity observed in 5′-PDβ2 constructs from which the distal sequences were deleted could suggest a more complex architecture in which a mixture of positive and negative effectors coordinately regulates the core 5′-PDβ2.

A role for germline promoters in controlling the recombination of downstream gene segments has been supported in the *Tcra* (20, 21, 24), *Tcrb* (19), *Tcr delta* (41), and *IgH* loci (22). Deletion of the J49α promoter selectively impaired assembly of J segments 3′ of the deletion without significantly affecting the recombination potential of upstream Js (21). Likewise, D-to-J recombination in stably transfected substrates was progressively attenuated by the repositioning of PDβ1 at increasing distances 3′ of Dβ1 (23). In light of the localization of germline promoter activity between Dβ2 and Jβ2.1, the effects of PDβ1 repositioning on DJ recombination bear a marked similarity to the relative inefficiency with which Dβ2Jβ2 joints are made in vivo (9–12). Alternatively, Dβ2 recombination levels relative to Dβ1 could reflect the presence of less efficient RSS sites within the DJCβ2 cassette, or a reduced ability of the Dβ2 region to recruit enhancer-dependent chromatin alteration. Our analyses of germline transcription argue against the possibility that Dβ2 accessibility is developmentally delayed until after T lineage commitment in DN2 cells (7).

What evolutionary advantage would drive the unique organization of Dβ2 promoter activity? D-to-J joints in *Tcrb* are rarely out of frame. By contrast, two in every three V-to-DJβ joints will contain a frameshift that renders the assembly nonfunctional. In New Zealand White mice that lack the DJβ2 gene segments, the frameshift potential of V-to-DJβ joining would theoretically block ~44% of early thymocytes from progressing through the αβ lineage beyond β selection. However, the positioning of two complete DJC cassettes downstream of the Vβ elements would offer each allele an attempt to rescue nonproductive V(D)J joints involving Dβ1. Such a selective advantage to αβ development would only be realized if the initial DJ substrates for Vβ recombination were preferentially assembled from the upstream DJ cassette, because V-to-DJβ2 rearrangements delete the Dβ1 sequences. Therefore, positioning of the germline promoter downstream of Dβ2 could provide the programmed inefficiency in DJβ2 rearrangement necessary to maximize the opportunities to assemble a functional *Tcrb* gene.

NF-κB activation by the pre-TCR has previously been shown to be essential for the survival and progression of DN thymocytes to the DP stage (42). Likewise, the RelA and p50 subunits of NF-κB are required for early lymphopoiesis, most likely providing protection against TNF-induced apoptosis (43). In contrast to such classical pathway-mediated activation, previous studies showed that RelA and p50 were both constitutively localized to the nucleus of wild-type (44) and RAG-2-deficient thymocytes, although at levels substantially below those in DP cells (45). Consistent with our findings in P5424, the levels of nuclear NF-κB were greatly diminished in DN thymocytes incubated in vitro at 37°C, but remained readily inducible by PMA and ionomycin (45). A potential role for NF-κB in 3′-PDβ2-mediated accessibility of Dβ2 to recombinase would seem to necessitate such constitutive nuclear localization. However, it is intriguing to consider whether the capacity to augment NF-κB levels in developing thymocytes might

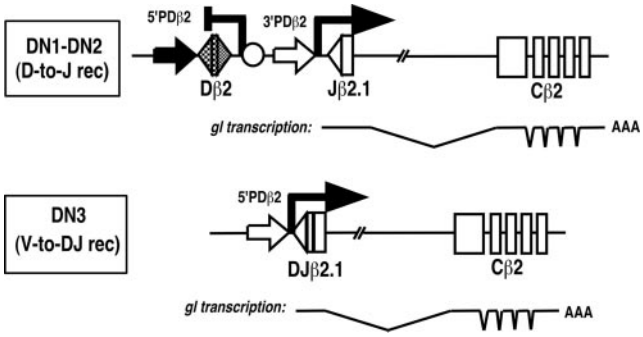


**FIGURE 8.** Model of transcriptional regulation at D$\beta$2. Schematic depictions of the germline (*top*) and assembled D$\beta$2 and J$\beta$2.1 gene segments (*bottom*). Block arrows and circle represent the 5′- and 3′-PD$\beta$2 promoters and 5′-PD$\beta$2 repressor element. Shading in the germline elements indicates partial (stippled) or complete transcriptional and recombinational inactivity (filled). The model proposes that repression of 5′-PD$\beta$2 during DN1/DN2 development relegates transcription of the DJ$\beta$2 gene segment cluster to the 3′-PD$\beta$2 promoter, which only weakly provides recombinational accessibility to the D$\beta$2 3′-RSS. Upon deletion of the repressor and 3′ promoter during D-to-J recombination, 5′-PD$\beta$2 is strongly activated and provides D$\beta$2 5′-RSS accessibility for V-to-DJ joining in DN3-staged cells.

allow for select stimuli to impact D$\beta$2 usage in the overall TCR$\beta$ repertoire.

The dependence of V$\beta$ recombination on formation of a DJ$\beta$ joint has limited study of the role promoters might play in V-to-DJ assembly. Nonetheless, the breadth of sequence that separates V$\beta$ elements from the DJC$\beta$ cassettes, together with the dependence of *Tcra* assembly on J$\alpha$ promoters (24), strongly suggests an analogous role for D$\beta$ germline promoter activity in V$\beta$-to-DJ$\beta$ assembly. Consequently, rearrangement of DJ$\beta$2 joints with upstream V$\beta$ elements would require that a second D$\beta$2 promoter reside upstream of D$\beta$2, and be active only after DJ assembly. Our finding that transcription initiates predominantly downstream of D$\beta$2 before recombination and upstream of DJ$\beta$2 joints (Fig. 2) corroborates longstanding Northern analyses in wild-type (4, 46) and RAG-deficient thymocytes (31), and strongly supports such a model in which dual promoters sequentially drive inefficient D-to-J joining and then V-to-DJ joining (Fig. 8).

It remains unclear how activity of the 5′-PD$\beta$2 promoter is limited before DJ$\beta$ recombination. Deletion studies suggest that elements within a 100- to 300-bp region between the two promoters selectively repress activity of the upstream promoter without affecting the downstream promoter (Fig. 3). Indeed, a similar cryptic repressive activity immediately downstream of D$\beta$1 was suggested to modestly impair PD$\beta$1 activity (34). EMSA confirmed binding sites for the Sp1 and GATA-3 transcription factors within the region of the putative 5′-PD$\beta$2 repressor (Fig. 5). Although Sp1 and GATA-3 have both been defined primarily as transcriptional activators, each has the capacity to drive transcriptional repression (47, 48). However, reporter constructs from which fragments containing the Sp1 and G3-5 and G3-6 sites had been deleted retained their ability to repress 5′-PD$\beta$2 activity (Fig. 3, –1104/+98). It remains to be seen whether either element contributes to repression of 5′-PD$\beta$2 activity in a chromatin setting. Indeed, many or all of the sites surrounding D$\beta$2 could function within the endogenous chromatin as part of a single complex that preferentially targets transcription start sites 3′ of D$\beta$2 until they are eliminated by D-to-J recombination. Alternatively, other as yet undefined elements between D$\beta$2 and J$\beta$2.1 may contribute to repression of the upstream promoter, or DJ recombination could relieve topological restraints that prevent occupancy of the upstream promoter. Oltz and colleagues (39) have recently shown that both Runx1- and TATA-binding protein are recruited to targets upstream of the unrearranged D$\beta$2 sequences in RAG-deficient thymocytes, and coordinate physical interaction between the D$\beta$2 and E$\beta$ elements. Their findings, coupled with the general openness of chromatin within the DJ$\beta$2 cassette of P5424 cells (49), argue against a model in which the upstream promoter is epigenetically silenced by chromatin condensation. Future studies will be necessary to unravel the complex regulatory schemes that govern differential promoter activation at D$\beta$2, and to assess the potential impact of each element on *Tcrb* assembly.

## Acknowledgments

We gratefully thank Dr. Michael Krangel for advice in preparing this manuscript; Drs. Jianzhu Chen and Pierre Ferrier for providing the C57BL/6, PD$\beta1^{-/-}$, and E$\beta^{-/-}$ mice and the P5424 cell line; Drs. Scott Laster and Jonathon Olson for key reagents; and Janet Dow at the Flow Cytometry and Cell Sorting Facility at North Carolina State University College of Veterinary Medicine.

## Disclosures

The authors have no financial conflict of interest.

## References

1. Schatz, D. G. 1989. The V(D)J recombination activating gene, RAG-1. *Cell* 59: 1035–1048.
2. Oettinger, M. A. 1990. RAG-1 and RAG-2, adjacent genes that synergistically activate V(D)J recombination. *Science* 248: 1517–1523.
3. Gellert, M. 2002. V(D)J recombination: RAG proteins, repair factors, and regulation. *Annu. Rev. Biochem.* 71: 101–132.
4. Godfrey, D. I., J. Kennedy, P. Mombaerts, S. Tonegawa, and A. Zlotnik. 1994. Onset of TCR-$\beta$ gene rearrangement and role of TCR-$\beta$ expression during $CD3^-CD4^-CD8^-$ thymocyte differentiation. *J. Immunol.* 152: 4783–4792.
5. Dudley, E. C., H. T. Petrie, L. M. Shah, M. J. Owen, and A. C. Hayday. 1994. T cell receptor $\beta$ chain gene rearrangement and selection during thymocyte development in adult mice. *Immunity* 1: 83–93.
6. Petrie, H. T., F. Livak, D. Burtrum, and S. Mazel. 1995. T cell receptor gene recombination patterns and mechanisms: cell death, rescue, and T cell production. *J. Exp. Med.* 182: 121–127.
7. King, A. G., M. Kondo, D. C. Scherer, and I. L. Weissman. 2002. Lineage infidelity in myeloid cells with TCR gene rearrangement: a latent developmental potential of pro-T cells revealed by ectopic cytokine receptor signaling. *Proc. Natl. Acad. Sci. USA* 99: 4508–4513.
8. Porritt, H. E., L. L. Rumfelt, S. Tabrizifard, T. M. Schmitt, J. C. Zuniga-Pflucker, and H. T. Petrie. 2004. Heterogeneity among DN1 prothymocytes reveals multiple progenitors with different capacities to generate T cell and non-T cell lineages. *Immunity* 20: 735–745.
9. Uematsu, Y., S. Ryser, Z. Dembic, P. Borgulya, P. Krimpenfort, A. Berns, H. von Boehmer, and M. Steinmetz. 1988. In transgenic mice the introduced functional T cell receptor $\beta$ gene prevents expression of endogenous $\beta$ genes. *Cell* 52: 831–841.
10. Born, W., J. Yague, E. Palmer, J. Kappler, and P. Marrack. 1985. Rearrangement of T-cell receptor $\beta$-chain genes during T-cell development. *Proc. Natl. Acad. Sci. USA* 82: 2925–2929.
11. Haars, R., M. Kronenberg, W. M. Gallatin, I. L. Weissman, F. L. Owen, and L. Hood. 1986. Rearrangement and expression of T cell antigen receptor and $\gamma$ genes during thymic development. *J. Exp. Med.* 164: 1–24.
12. Lindsten, T., B. J. Fowlkes, L. E. Samelson, M. M. Davis, and Y. H. Chien. 1987. Transient rearrangements of the T cell antigen receptor $\alpha$ locus in early thymocytes. *J. Exp. Med.* 166: 761–775.
13. Krangel, M. S. 2003. Gene segment selection in V(D)J recombination: accessibility and beyond. *Nat. Immunol.* 4: 624–630.
14. Cobb, R. M., K. J. Oestreich, O. A. Osipovich, and E. M. Oltz. 2006. Accessibility control of V(D)J recombination. *Adv. Immunol.* 91: 45–109.
15. Bories, J. C., J. Demengeot, L. Davidson, and F. W. Alt. 1996. Gene-targeted deletion and replacement mutations of the T-cell receptor $\beta$-chain enhancer: the role of enhancer elements in controlling V(D)J recombination accessibility. *Proc. Natl. Acad. Sci. USA* 93: 7871–7876.
16. Bouvier, G., F. Watrin, M. Naspetti, C. Verthuy, P. Naquet, and P. Ferrier. 1996. Deletion of the mouse T-cell receptor $\beta$ gene enhancer blocks $\alpha\beta$ T-cell development. *Proc. Natl. Acad. Sci. USA* 93: 7877–7881.
17. Hempel, W. M., P. Stanhope-Baker, N. Mathieu, F. Huang, M. S. Schlissel, and P. Ferrier. 1998. Enhancer control of V(D)J recombination at the TCR$\beta$ locus: differential effects on DNA cleavage and joining. *Genes Dev.* 12: 2305–2317.
18. Sikes, M. L., C. C. Suarez, and E. M. Oltz. 1999. Regulation of V(D)J recombination by transcriptional promoters. *Mol. Cell. Biol.* 19: 2773–2781.
19. Whitehurst, C. E., S. Chattopadhyay, and J. Chen. 1999. Control of V(D)J recombinational accessibility of the D$\beta$1 gene segment at the TCR$\beta$ locus by a germline promoter. *Immunity* 10: 313–322.

20. Villey, I., D. Caillol, F. Selz, P. Ferrier, and J. P. de Villartay. 1996. Defect in rearrangement of the most 5′ TCR-Jα following targeted deletion of T early α (TEA): implications for TCRα locus accessibility. *Immunity* 5: 331–342.
21. Hawwari, A., C. Bock, and M. S. Krangel. 2005. Regulation of T cell receptor α gene assembly by a complex hierarchy of germline Jα promoters. *Nat. Immunol.* 6: 481–489.
22. Afshar, R., S. Pierce, D. J. Bolland, A. Corcoran, and E. M. Oltz. 2006. Regulation of IgH gene assembly: role of the intronic enhancer and 5′DQ52 region in targeting DHJH recombination. *J. Immunol.* 176: 2439–2447.
23. Sikes, M. L., A. Meade, R. Tripathi, M. S. Krangel, and E. M. Oltz. 2002. Regulation of V(D)J recombination: a dominant role for promoter positioning in gene segment accessibility. *Proc. Natl. Acad. Sci. USA* 99: 12309–12314.
24. Abarrategui, I., and M. S. Krangel. 2006. Regulation of T cell receptor-α gene recombination by transcription. *Nat. Immunol.* 7: 1109–1115.
25. Sikes, M. L., R. J. Gomez, J. Song, and E. M. Oltz. 1998. A developmental stage-specific promoter directs germline transcription of DβJβ gene segments in precursor T lymphocytes. *J. Immunol.* 161: 1399–1405.
26. Mombaerts, P., C. Terhorst, T. Jacks, S. Tonegawa, and J. Sancho. 1995. Characterization of immature thymocyte lines derived from T-cell receptor or recombination activating gene 1 and p53 double mutant mice. *Proc. Natl. Acad. Sci. USA* 92: 7420–7424.
27. Lee, N. E., and M. M. Davis. 1988. T cell receptor β-chain genes in BW5147 and other AKR tumors: deletion order of murine Vβ gene segments and possible 5′ regulatory regions. *J. Immunol.* 140: 1665–1675.
28. Kim, K. J., C. Kanellopoulos-Langevin, R. M. Merwin, D. H. Sachs, and R. Asofsky. 1979. Establishment and characterization of BALB/c lymphoma lines with B cell properties. *J. Immunol.* 122: 549–554.
29. Ciccone, D. N., K. B. Morshead, and M. A. Oettinger. 2004. Chromatin immunoprecipitation in the analysis of large chromatin domains across murine antigen receptor loci. *Methods Enzymol.* 376: 334–348.
30. Malissen, M., A. Gillet, L. Ardouin, G. Bouvier, J. Trucy, P. Ferrier, E. Vivier, and B. Malissen. 1995. Altered T cell development in mice with a targeted mutation of the CD3-ε gene. *EMBO J.* 14: 4641–4653.
31. Whitehurst, C. E., M. S. Schlissel, and J. Chen. 2000. Deletion of germline promoter PDβ1 from the TCRβ locus causes hypermethylation that impairs Dβ1 recombination by multiple mechanisms. *Immunity* 13: 703–714.
32. Chattopadhyay, S., C. E. Whitehurst, F. Schwenk, and J. Chen. 1998. Biochemical and functional analyses of chromatin changes at the TCR-β gene locus during $CD4^-CD8^-$ to $CD4^+CD8^+$ thymocyte differentiation. *J. Immunol.* 160: 1256–1267.
33. Smale, S. T., and J. T. Kadonaga. 2003. The RNA polymerase II core promoter. *Annu. Rev. Biochem.* 72: 449–479.
34. Doty, R. T., D. Xia, S. P. Nguyen, T. R. Hathaway, and D. M. Willerford. 1999. Promoter element for transcription of unrearranged T-cell receptor β-chain gene in pro-T cells. *Blood* 93: 3017–3025.
35. Gottschalk, L. R., and J. M. Leiden. 1990. Identification and functional characterization of the human T-cell receptor β gene transcriptional enhancer: common nuclear proteins interact with the transcriptional regulatory elements of the T-cell receptor α and β genes. *Mol. Cell. Biol.* 10: 5486–5495.
36. Marine, J., and A. Winoto. 1991. The human enhancer-binding protein Gata3 binds to several T-cell receptor regulatory elements. *Proc. Natl. Acad. Sci. USA* 88: 7284–7288.
37. Merika, M., and S. H. Orkin. 1993. DNA-binding specificity of GATA family transcription factors. *Mol. Cell. Biol.* 13: 3999–4010.
38. Rothenberg, E. V., and T. Taghon. 2005. Molecular genetics of T cell development. *Annu. Rev. Immunol.* 23: 601–649.
39. Oestreich, K. J., R. M. Cobb, S. Pierce, J. Chen, P. Ferrier, and E. M. Oltz. 2006. Regulation of TCRβ gene assembly by a promoter/enhancer holocomplex. *Immunity* 24: 381–391.
40. Patenge, N., S. K. Elkin, and M. A. Oettinger. 2004. ATP-dependent remodeling by SWI/SNF and ISWI proteins stimulates V(D)J cleavage of 5 S arrays. *J. Biol. Chem.* 279: 35360–35367.
41. Carabana, J., E. Ortigoza, and M. S. Krangel. 2005. Regulation of the murine Dδ2 promoter by upstream stimulatory factor 1, Runx1, and c-Myb. *J. Immunol.* 174: 4144–4152.
42. Voll, R. E., E. Jimi, R. J. Phillips, D. F. Barber, M. Rincon, A. C. Hayday, R. A. Flavell, and S. Ghosh. 2000. NF-κB activation by the pre-T cell receptor serves as a selective survival signal in T lymphocyte development. *Immunity* 13: 677–689.
43. Siebenlist, U., K. Brown, and E. Claudio. 2005. Control of lymphocyte development by nuclear factor-κB. *Nat. Rev. Immunol.* 5: 435–445.
44. Weih, F., D. Carrasco, and R. Bravo. 1994. Constitutive and inducible Rel/NF-κB activities in mouse thymus and spleen. *Oncogene* 9: 3289–3297.
45. Sen, J., L. Venkataraman, Y. Shinkai, J. W. Pierce, F. W. Alt, S. J. Burakoff, and R. Sen. 1995. Expression and induction of nuclear factor-κB-related proteins in thymocytes. *J. Immunol.* 154: 3213–3221.
46. Siu, G., M. Kronenberg, E. Strauss, R. Haars, T. W. Mak, and L. Hood. 1984. The structure, rearrangement and expression of Dβ gene segments of the murine T-cell antigen receptor. *Nature* 311: 344–350.
47. Won, J., J. Yim, and T. K. Kim. 2002. Sp1 and Sp3 recruit histone deacetylase to repress transcription of human telomerase reverse transcriptase (hTERT) promoter in normal human somatic cells. *J. Biol. Chem.* 277: 38230–38238.
48. Usui, T., R. Nishikomori, A. Kitani, and W. Strober. 2003. GATA-3 suppresses Th1 development by down-regulation of Stat4 and not through effects on IL-12Rβ2 chain or T-bet. *Immunity* 18: 415–428.
49. Morshead, K. B., D. N. Ciccone, S. D. Taverna, C. D. Allis, and M. A. Oettinger. 2003. Antigen receptor loci poised for V(D)J rearrangement are broadly associated with BRG1 and flanked by peaks of histone H3 dimethylated at lysine 4. *Proc. Natl. Acad. Sci. USA* 100: 11577–11582.